

Raman Spectroelectrochemistry of Polyaniline Synthesized Using Different Electrolytic Regimes – Multivariate Analysis[#]

Maria Grzeszczuk*, Anna Grańska, Roman Szostak

Faculty of Chemistry, University of Wrocław, F. Joliot-Curie 14, 50-383 Wrocław, Poland

*E-mail: maria.grzeszczuk@chem.uni.wroc.pl

Received: 8 May 2013 / Accepted: 16 June 2013 / Published: 1 July 2013

Potentiostatic, galvanostatic and cyclic potentiodynamic depositions of polyaniline were studied by cyclic voltammetry and *in-situ* Raman spectroscopy. Multivariate analysis of the spectroelectrochemical data including evolving factor analysis, multivariate curve resolution and 2D-correlation spectroscopy was applied to resolve overlapped bands in Raman spectra and to assign them reliably. Oxidized structures, related with a different chemical composition of the polymer chains, were evidenced in the leucoemeraldine ↔ emeraldine process with their proportions changing in the order: potentiostatic > galvanostatic > potentiodynamic. Both techniques, cyclic voltammetry and Raman spectroscopy indicate the most complex nature of the polymer films produced under the galvanostatic regime of electrolysis.

Keywords: polyaniline, electrochemical synthesis, cyclic voltammetry, Raman spectroscopy, multivariate analysis

[#] Presented at ISE Satellite Meeting “Spectroelectrochemistry 2012”, 26-29 August 2012, Dresden, Germany

1. INTRODUCTION

Impact of various chemical and electrical factors on electrosynthesis and resulting properties of conducting polymers like polyaniline (PANI) was studied thoroughly [1,2]. The studies reported had focused on substrate electrode material, electrode potential, current density, effects of solvent and ionic composition of supporting electrolyte. The influence of structural morphology of the substrate electrode surface on electrochemical properties and structure of the formed polymer film was also recognised [3,4].

In situ Raman spectroscopic studies of the PANI redox transitions were reported for different excitation wavelengths including the blue (458 nm), the red (676 nm) and near-infrared excitation

(1064 nm). As the resonance Raman conditions are not the same for distinct oxidation states and protonation levels the resulting spectra differ strongly [5-10]. The semiquinone radical structures arising in the electrochemical leucoemeraldine – emeraldine process can be best observed using the red or infrared excitation lines [6].

As the intermediate cation-radical species of the polymer oxidation were expected to be sensitive to a nature of counterions we had undertaken a search of molecular factors important for the dynamics of the polymer redox transformation using cyclic voltammetry, electrochemical impedance spectroscopy and Raman measurements on thin PANI layers electrodeposited and undergoing redox state switching in a presence of different acids, including a family of trihalogenoacetic acids [11-14]. The Raman studies confirmed that the magnitude of redox switching hysteresis is correlated with the polymer structure monitored via the polaron vibrational bands of PANI [14].

A goal of this work is to show consequences of three main regimes of electrosynthesis, namely potentiostatic, galvanostatic and cyclic potentiodynamic, applied in comparable potential and current windows, for composition and structure of electrodeposited PANI by using simultaneously *in-situ* Raman spectroscopy and cyclic voltammetry. Thus, by combining information from the electrosynthesis process and the two methods of the product identification, the chemical composition of the polymer samples can be viewed, hopefully, in terms of possible differences in mean conjugation length, chain packing structure, average oxidation and protonation levels of the PANI deposit. We are going to show that cyclic voltammetry and potentiostatic step Raman spectroelectrochemistry can provide complementary information on the polymer in a course of its redox switching. Mechanistic, kinetic and compositional complexities of the monitored processes and states may cause serious misinterpretation when only one method is chosen to characterize the sample. Our purpose is to show that a combination of the dynamic electrochemical method and Raman spectroscopy may lead to a more credible characterization and comparison of the PANI samples obtained at different electrical regimes of electropolymerization. Effects of galvanostatic, potentiostatic and potentiodynamic synthesis monitored by *in-situ* Raman spectroscopy of the polymeric product had not been reported before.

The electrochemical synthesis and redox transformations of PANI were performed at polycrystalline platinum, in aqueous sulfuric acid which is the supporting electrolyte used commonly for fundamental studies and applications. Differences in adsorption of ions and molecules at the metal and the polymer modified surface, a change in pH at the reaction place due to the electrode potential and undergoing electrode reactions can induce differences in intermolecular bonding thus influencing the chemical composition as well as conformation and packing of the polymer chains. It is worth to notice that activity and acidity of aqueous sulfuric acid has been discussed thoroughly recently [15].

The chemical identification of the insoluble polymer product may not be an easy task because the polymer film is a mixture of macromolecules as well as amorphous-crystalline regions. To resolve overlapped bands in Raman spectra obtained for the PANI products, different techniques of multivariate analysis including evolving factor analysis (EFA) [16], multivariate curve resolution (MCR) [17], and mainly 2D-correlation spectroscopy (2D-COS) [18,19] were applied to the recorded spectroelectrochemical data sets. There are scarce examples of EFA and MCR analysis of UV-Vis spectroelectrochemical data [20-22] and even more rare in the case of two-dimensional correlation

spectroscopy [21,23] although application of EFA, MCR and 2D-COS analysis in vibrational and optical spectroscopy is widely recognised [16-19,24-26]. Electrochemical deposition of polyaniline was analyzed using UV-Vis spectroelectrochemistry aided by the 2D-COS and MCR analysis [21].

2. EXPERIMENTAL

2.1. Electrodes

Working electrode: a polycrystalline Pt (disc, $A_{\text{geom.}} = 0.07 \text{ cm}^2$, Metrohm); auxiliary electrode: glassy carbon (rod, Metrohm); reference electrode: SCE (+0.23 V vs. SHE). The Pt electrode was subjected to a mechanical cleaning/polishing using Al_2O_3 powders in order of a decreasing size of the grains (10, 3, 1, 0.3, 0.03 μm), during 5 minutes for the each step. Polyaniline was removed before the polishing by immersing in a Pirantha mixture and sonification. After cleaning and polishing, the working Pt electrode was treated electrochemically by cycling at 50 mV/s in aqueous 0.5 M H_2SO_4 in a potential window encompassing the oxide formation/removal and the onset of the hydrogen evolution.

2.2. Solutions

Electropolymerization of aniline: aqueous 0.5 M aniline in 0.5 M H_2SO_4 ; electrochemical and spectroscopic characterization of PANI: aqueous 0.5 M H_2SO_4 . A nitrogen steam was used to drive away oxygen from the solutions and a contacting atmosphere.

2.3. Chemicals

Aniline (POCH, p.a.) was doubly distilled at a reduced pressure and under nitrogen; sulfuric acid (POCH, 95%, p.a.), water (Millipore) and nitrogen (purity > 99.999 %) were used.

2.4. Apparatus

An Autolab instrument with GPES v. 4.8 software (Eco-Chemie) was used for electrochemical syntheses by applying protocols of chronoamperometry, chronopotentiometry and cyclic voltammetry (cv). This apparatus was also utilized for redox switching characterization of the polymer (cv), and to control its redox state during *in-situ* spectroscopic measurements (chronoamperometry). Raman spectra were registered using a Magna 860 FT-IR spectrometer (Thermo Nicolet) equipped with a CaF_2 beamsplitter and interfaced with a FT Raman accessory. The thin PANI films on Pt electrodes, situated nearly perpendicularly to the laser beam, were illuminated by Nd:YVO₄ laser ($\lambda = 1064 \text{ nm}$) with a power of 400 mW at a sample, without the converging lens. The backscattered radiation was collected. The interferograms were recorded by a InGaAs detector, averaged over 1280 scans, Happ-

Genzel apodised and Fourier transformed using a zero filling factor of 2 to give spectra in the 100–3700 cm^{-1} range, at a resolution of 4 cm^{-1} .

2.5. Procedures

Electrodeposition of aniline was performed using three regimes of polarization of the platinum electrode: 1) potentiostatic at 0.75 V, 2) potentiodynamic at $\langle 0.75\text{V}, -0.1\text{V} \rangle$ potential range, and galvanostatic resulting in $\langle 0.76\text{V}, 0.61\text{V} \rangle$ potential range; where the potentials are expressed in the SCE scale. The produced PANI films were of submicrometer thicknesses what was estimated based on the charge involved in the reversible redox switching of the polymer deposits [11]. Raman spectra were recorded at eight values of the electrode potential in the reduction direction, $(+0.5, +0.4, +0.3, +0.2, +0.1, 0.0, -0.1, -0.2 \text{ V})$, corresponding to the reversible redox states of the emeraldine/leukoemeraldine system in the strong acid. Additionally, selected spectra were recorded for the oxidation direction to check the reversibility of the redox states.

3. RESULTS AND DISCUSSION

3.1. Electrodeposition

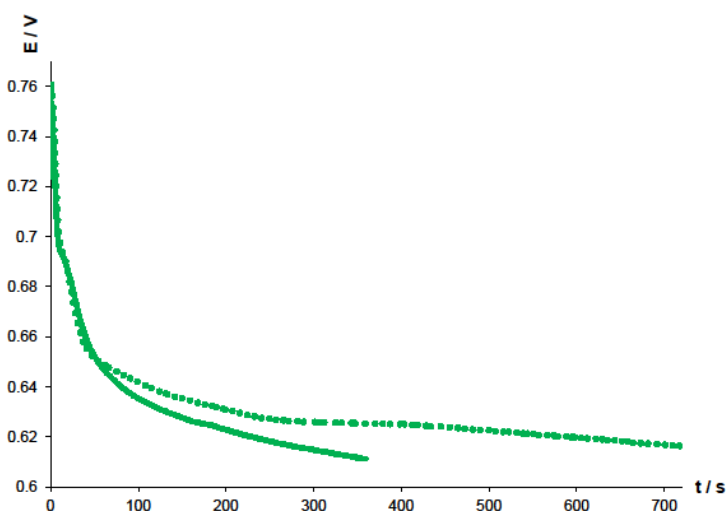


Figure 1. Chronopotentiograms of galvanostatic electropolymerization of aniline at Pt in aqueous 0.5 M aniline - 0.5 M H_2SO_4 for two films of polyaniline. Current density was 0.5 mA/cm^2

Chronoamperograms and chronopotentiograms recorded during the electropolymerization provide easy tools for testing reproducibility of the process. It was observed that using the same substrate electrodes, surface purification methods, solutions for polymerization process, the current – time and potential – time curves were not the same when compared on a strictly quantitative basis. The irreproducibility of an initial stage of electropolymerization in the case of the potentiostatic

synthesis as well as final stages of electropolymerization in the case of the galvanostatic synthesis was observed (Fig. 1). Certainly, the cyclic voltammograms of electropolymerization process are not fully quantitatively reproducible also, however, the differences in the corresponding current – potential curves are not seen so easy as in chronoamperograms and chronopotentiograms, especially without processing the raw cv data. Noteworthy, the cyclic potentiodynamic regime of electrochemical deposition of PANI is used the most frequently. The electrical parameters of the three electrolytic regimes were selected to minimize the potential and current windows of the three methods. Therefore, the maximal deposition rates were similar with the three methods.

It has already been recognized that an electrical regime of electrosynthesis influences properties of deposited PANI but the electrodeposited polymeric products have not been characterized yet in terms of differences in chemical composition and structure [27,28]. Raman spectroscopy is the method of choice to look deeper into the matter. Cyclic voltammetry is used in this work to test stability of the redox response and to find correlations between Raman spectral features and redox properties of electrochemically synthesized PANI.

3.2. Electrochemistry of deposited polyaniline

Representative cyclic voltammograms of PANI films of a similar thickness, prepared using the three methods of electrosynthesis are shown in Fig. 2.

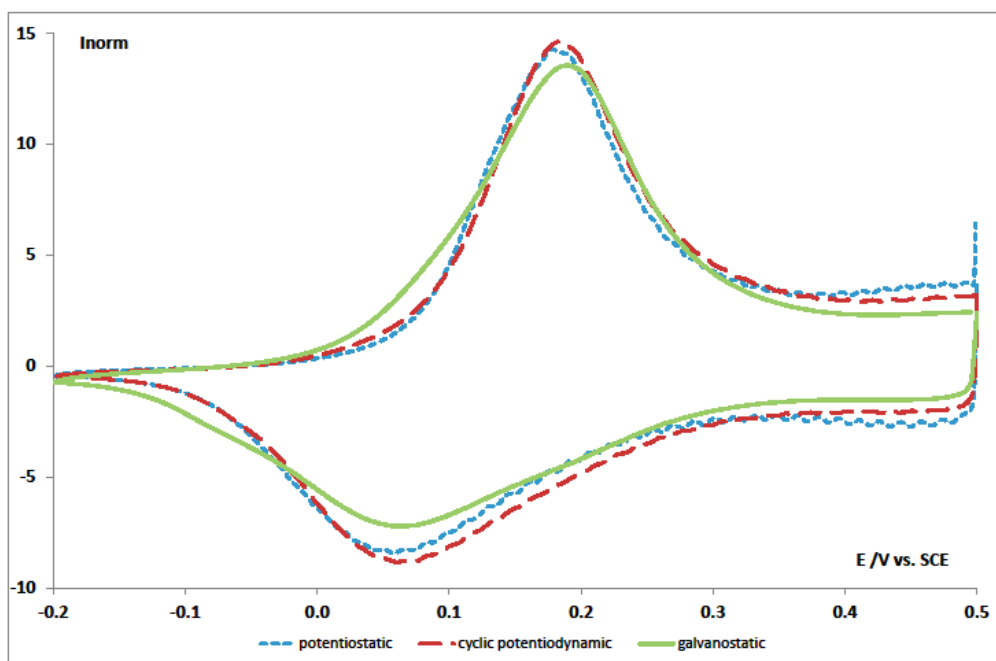


Figure 2. Thickness normalized cyclic voltammograms of polyaniline in aqueous 0.5 M sulfuric acid. Film thicknesses estimated based on the cathodic redox charge: potentiostatic (0.3 μm), potentiodynamic (0.3 μm), galvanostatic (0.4 μm)

The cv characteristics of the galvanostatic PANI indicates its higher inhomogeneity (*vide* peak widths) in comparison with PANI samples synthesized under the electrode potential control. A lower mean conjugation length (*vide* peak positions) and possibly a lower oxidation degree, as can be

inferred from peak and redox plateau currents, of the galvanostatic film might be true as well. The observed behaviour arises from many causes related to the polymer chain structure/composition. An additional impact on the composition/structure of the polymer can originate from the differences in sulfate and bisulfate adsorption on platinum that would influence the very first layers of the polymer deposit. *In situ* FT-IR studies of the asymmetric $\nu(\text{SO}_4)$ stretching and the bending mode in H_2O of species adsorbed at platinum electrode from aqueous 0.5 M sulfuric acid had revealed coadsorption of sulfate (SO_4^{2-}) and bisulfate (HSO_4^-) ions [29]. In the double layer region of the platinum electrode, the band intensity ratio of the two coadsorbed anions is much larger than in the solution bulk and it diminishes at potentials starting from 0.6 V up to 1.1 V vs. SCE, the adsorption of SO_4^{2-} gradually vanishes so the oxygenated platinum surface is getting covered solely by HSO_4^- and H_2O bonded to the oxide by the hydrogen bonds. It implies that the very first insoluble oligomeric species deposited galvanostatically on the platinum electrode may be doped with sulfate ions at a higher degree than those deposited potentiodynamically, what would depend on potential scan rate, and certainly than those deposited potentiostatically. Cyclic voltammetry shows distinct differences of the galvanostatic PANI as compared to the other ones (see Fig. 2). The most important feature of galvanostatically deposited PANI is a broader distribution of chain or conjugation lengths in this polymer featured by the highest width of the cv peaks.

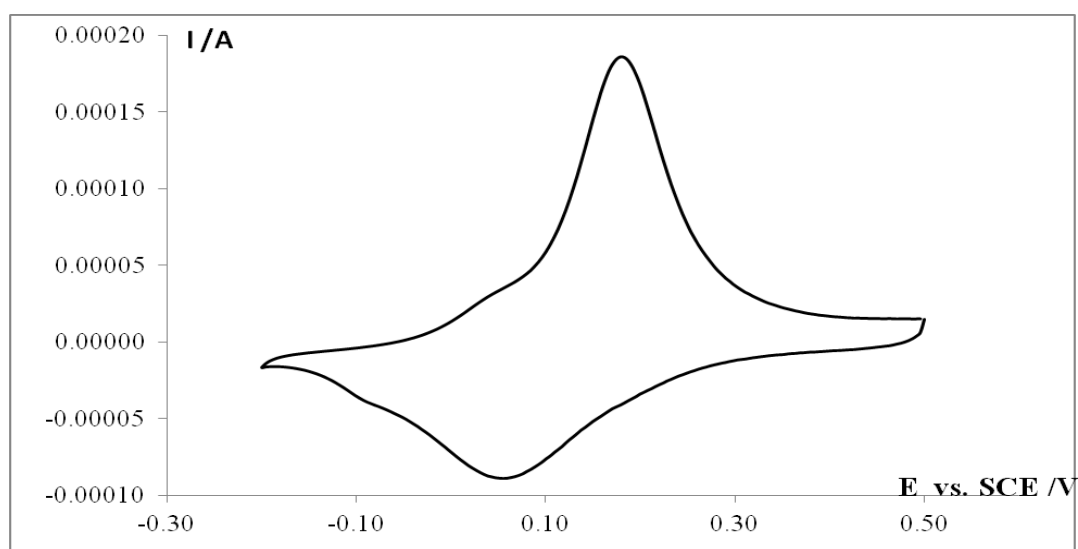


Figure 3. Cyclic voltammogram of the galvanostatic polyaniline ($0.1\mu\text{m}$) in aqueous 0.5 M H_2SO_4 at 50 mV/s

Cyclic voltammetry provides evidence for the specific structure or composition of a part of the galvanostatic deposit – distinct anodic/cathodic humps are observed for a thinner galvanostatic film at a negative side of the main peaks as shown in Fig. 3. It points out for a qualitative specificity of the very first chains of PANI, which can be either deposited on oxygenated surface of platinum and doped with HSO_4^- or, quite opposite, deposited on bare platinum and at least partly doped with SO_4^{2-} . The position of that small redox feature indicates that the polymer chains undergoing the observed process provide a longer mean conjugation length as compared to the overall polymer deposit as the specific

redox capacitance of the galvanostatic PANI with the lowest thickness (0.1 μm) is higher than obtained for the polymer synthesized at the other two regimes. Furthermore, the more negative redox processes of the main redox waves of conducting polymers are often due to complexity in ionic composition of a polymer film [1].

3.3. Spectroelectrochemistry of deposited polyaniline

At the first glance *in-situ* Raman spectra of the electrodeposited PANI seem not to be very sensitive to the experimental conditions applied for the electrochemical deposition. The spectra of emeraldine taken at 0.5 V for the different samples, shown in Fig. 4, look quite similar except for the Raman spectra of two galvanostatic PANI samples which differ in an intensity ratio of spectral components in the 1310-1380 cm^{-1} range.

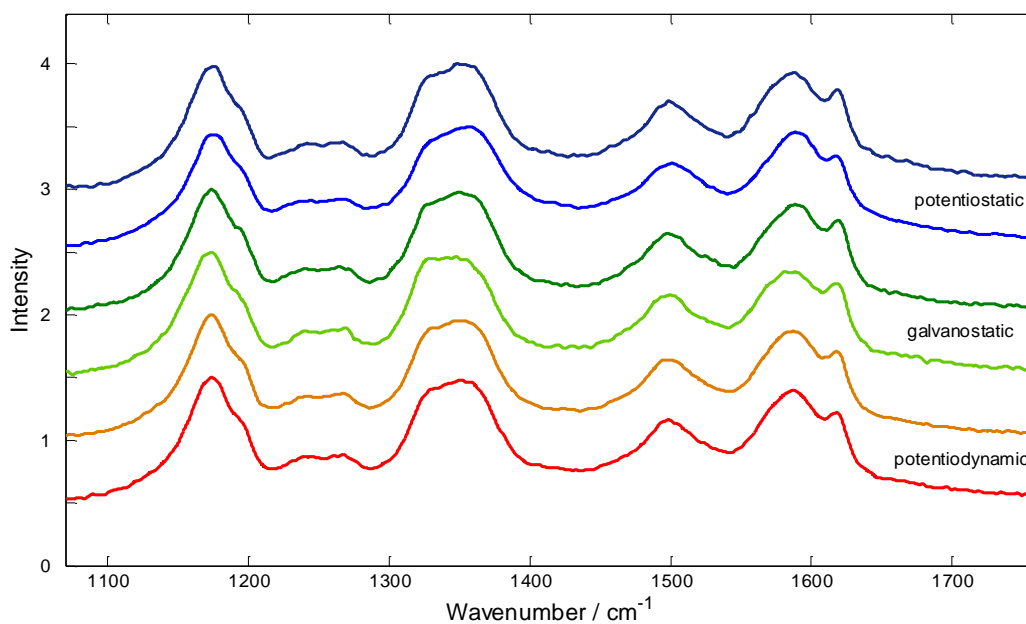


Figure 4. Raman spectra of individual submicrometer films of polyaniline recorded at 0.5 V in 0.5 M aqueous sulfuric acid

Assignments of spectral features to the vibrations of particular moieties were done on a basis of the literature data [4-10]. Raman spectra obtained with the 1064 nm line, recorded for the reversible emeraldine – leucoemeraldine transition are dominated by the $\nu(\text{CC})$ band at c.a. 1600 cm^{-1} , the imine $\nu(\text{C}=\text{N})$ and $\delta(\text{NH})$ vibration band with the maximum near 1500 cm^{-1} , the semibenzenoid polaronic $\nu(\text{C}\sim\text{N}^+)$ band at c.a. 1350 cm^{-1} , and the band of CH in plane bending vibration below 1200 cm^{-1} . The electrical regime of electropolymerization was found to influence only very slightly the Raman spectra peaks' positions of the resulting thin layer polymer product. The protonated semiquinone radical structure vibrations resonate with the near-infrared excitation radiation so the Raman bands of semiquinone polaronic $\nu(\text{C}\sim\text{N}^+)$ stretching modes are enhanced and thus any changes due to the

method of electropolymerization should be easier to follow. The polaronic band position and intensity depends on: 1) conjugation length of π -electrons in the chain causing shift to a lower energy and an intensity increase for a more extended conjugation, 2) degree of protonation of the chain - bands due to protonated and less protonated forms in the leucoemeraldine-emeraldine transition overlap and the later is situated at a higher energy, 3) so called symmetric ($C\sim N^{+}\sim C$) and non-symmetric ($C\sim N^{+}-C$) polaronic bonds that means equivalent and non-equivalent neighbour polaronic bonds, i.e. the bonds in the inner and the outer sites of the conjugated chain segment, respectively. The symmetric polaronic vibration band is situated at a lower energy than the non-symmetric one and a ratio of intensities of the two contributions should increase with conjugation length/chain length [30]. The terminal rings of the conjugated chain compared with the inner rings are little perturbed by oxidation and reveal a strong aromatic character. Therefore bands of $\nu(CC)$ and $\nu(CN^{+})$ vibrations ought to be the most appropriate for tracing of distinctions in conjugation length and oxidation level of PANI.

The observed differences in the Raman bands of $\nu(C\sim N^{+})$ as well as $\nu(CC)$ vibrations between the two galvanostatic samples point out effects of the film thickness, the thicker galvanostatic PANI layer seems to be more oxidized than the thinner one. This phenomenon was reported for polypyrrole [31].

Raman study on the kinetics of electrochemical degradation of PANI revealed that holding the PANI electrode at potential +0.8 V vs. Ag/AgCl, causes no significant qualitative modifications in the Raman spectra except for the observed changes in the relative intensities of some peaks. The behavior concerns the overlapping $\nu(CC)$ stretching bands in quinoid and semibenzenoid rings, with maxima at 1595 and 1630 cm^{-1} , respectively [32]. An increase of a relative intensity of the lower energy band as compared to the higher energy band was found with a time of the polarization, thus indicating an increase in the number of quinone type rings. Changes evolving with time were observed also in the region of the polaron band [32]. Therefore, the spectral differences observed for our two galvanostatic samples might originate from different levels of degradation of the two polymer samples also.

3.4. Multivariate analysis

Evidently different conditions of the preparative electrolysis impact properties of synthetic PANI, however, the resulted spectra are strongly convoluted and difficult to resolve. To make reliable assignment possible two chemometric methods EFA and MCR were used and the results compared with the 2D-COS analysis [16-19]. The characteristic spectral region 1100 -1700 cm^{-1} , containing the most prominent bands, was chosen for a quantitative analysis.

At first, a set of the mean Raman spectra for the each particular potential (six spectra were averaged, two for each of the three synthesis methods) was analyzed using standard methods. The selected spectral bands correspond to the $\delta(CH)$ in-plane bending, $\nu(C\sim N^{+})$, $\nu(C=N)/\delta(NH)$ and $\nu(CC)$ modes (upper panel of Fig. 5). Upon changes in the redox state a minimum of the bandwidth at the intermediate state for the bands connected with nitrogen atom motion and an increase of the bandwidth on oxidation for the other two bands was observed (lower panel of Fig. 5).

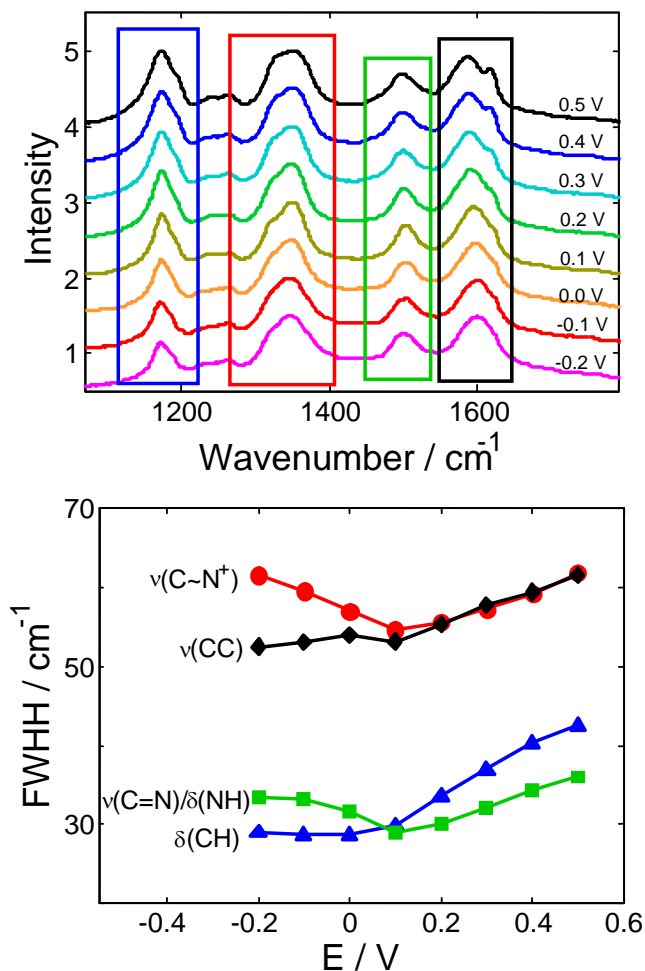


Figure 5. Mean Raman spectra of polyaniline films with the analyzed regions indicated by rectangles (top). The full width at half height for the $\delta(\text{CH})$ in-plane bending, superimposed $\nu(\text{C}=\text{N})$ stretching and $\delta(\text{NH})$ bending, $\nu(\text{C}\sim\text{N}^+)$ stretching, and $\nu(\text{CC})$ stretching bands (bottom)

Subsequently, the multivariate analysis of the mean Raman spectra involving EFA and then MCR was performed to resolve overlapped peaks into individual components. The procedure generated spectral and concentration profiles for the analyzed bands. The results for the $\nu(\text{CC})$ vibration band are shown in Fig. 6. EFA allows detection of the number of individual components present [16]. Three such components can be considered (please notice curves located above a noise level in Fig. 6A). However, only two of them can be resolved by MCR [17] at an acceptable level of accuracy. Therefore only the two spectral profiles are shown in Fig. 6B and the two concentration profiles are shown in Fig. 6C. They account for more than 95 % of variation in the analyzed set of spectra. They can be assigned to the intermediate (blue color) and oxidized (red color) polymer being semibenzenoid and quinoid structures, respectively (Figs. 6B, 6C). The profiles for the reduced form cannot be determined reliably because in the range of its presence measurements were performed only at electrode potential -0.1 and -0.2 V.

The other method of analysis available, which is independent from the combined EFA-MCR analysis, is the 2D correlation spectroscopy [18,19]. The asynchronous spectrum for the $\nu(\text{CC})$ vibration region is shown as a map (Fig. 6D). The correlating components have a similar shape in the correlation map. The reddish colors indicate a spectral component increasing concentration with oxidation, the bluish colors – a component decreasing concentration with potential. Magnitudes of the spectral changes are depicted by intensity of the colors. The 2D-COS spectrum for the $\nu(\text{CC})$ band indicates two main components at about 1580 and 1600 cm^{-1} , for the quinoid and semibenzenoid components, respectively. Another oxidized component is detected at about 1620 cm^{-1} , again correlating with the semibenzenoid component at 1600 cm^{-1} . The results obtained by two independent multivariate analysis methods, namely MCR and 2D-COS, are compatible.

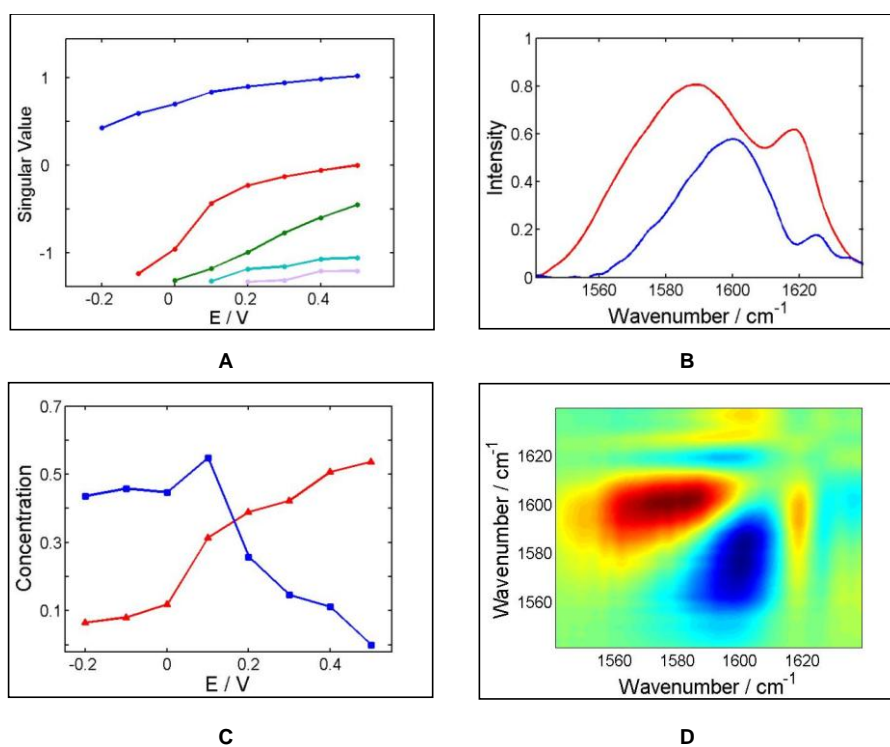


Figure 6. EFA profiles (A), MCR spectral profiles (B), MCR concentration profiles (C) and 2D-COS asynchronous map (D) for the $\nu(\text{CC})$ band of PANI resulted from the analysis of the mean spectra

3.5. Influence of electrosynthesis conditions

Changes in the spectra of the polymeric product due to the regime of electrosynthesis are presented as 2D-COS maps and MCR spectral profiles in Figs. 7-10. Two sets of spectra recorded for independent samples obtained for each of the electrosynthesis regime were first averaged and then used in the analysis.

The maps and the profiles for $\delta(\text{CH})$ in-plane deformation band (Fig. 7) indicate dominant contribution from the intermediate semibenzenoid state and coexistence of two oxidized spectral components.

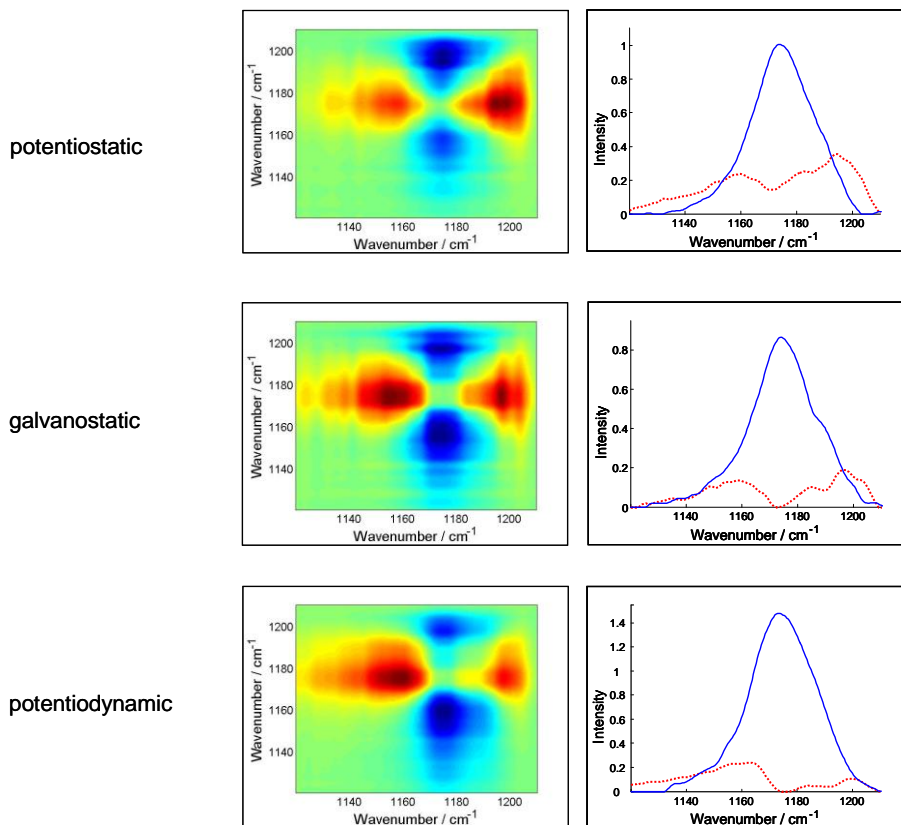


Figure 7. 2D-COS maps and MCR spectral profiles for the $\delta(\text{CH})$ in-plane bending band of electrodeposited PANI

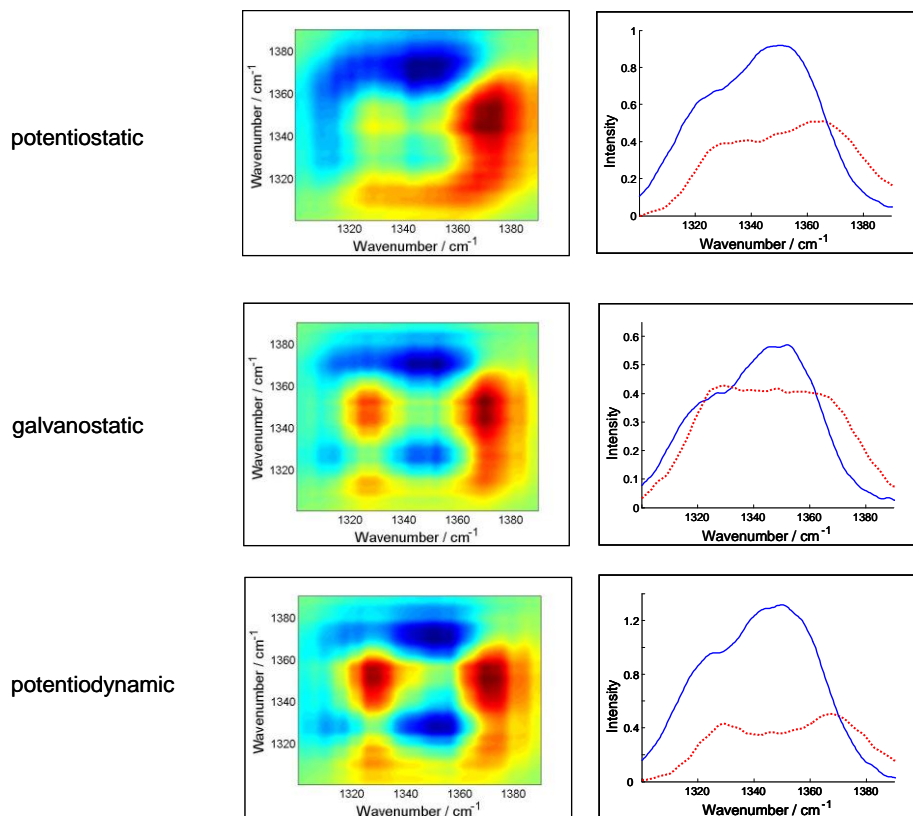


Figure 8. 2D-COS maps and MCR spectral profiles for the $\nu(\text{C}\sim\text{N}^+)$ stretching band of electrodeposited PANI

The potentiostatically synthesized polymer is richer in oxidized structure characterized by the 1200 cm^{-1} peak but the 1160 cm^{-1} peak is dominating in the potentiodynamic polymer. The galvanostatic synthesis results in a more equal content of the two components.

For the broad polaron band (Fig. 8) similar tendency is found as for the $\delta(\text{CH})$ band. The oxidation of the polymer increases contribution from the lower energy oxidized structure in the following order: potentiostatic < galvanostatic < potentiodynamic. Furthermore, the highly overlapping spectral contributions of the potentiostatic PANI have separated into the low energy components for the galvanostatic and potentiodynamic samples. The differences result probably from different contributions of the various charged states of the protonated and unprotonated structures of emeraldine (polarons, π -dimers, polaron pairs) [33,34].

The complex band composed of the imine $\nu(\text{C}=\text{N})$ stretching at 1480 cm^{-1} and the $\delta(\text{NH})$ bending contributions at near 1500 cm^{-1} is dominated by the lower energy oxidized structure (Fig. 9). The potentiodynamic synthesis produces the most homogeneous polymer exhibiting the most homogeneous spectral characteristics of the two main peaks. Noteworthy, the overall pattern for this band is changing in the similar way to the other bands under the analysis.

The $\nu(\text{CC})$ stretching band (Fig. 10) is composed of the quinoid $\nu(\text{C}=\text{C})$ peaks at 1580 and 1620 cm^{-1} . The semibenzenoid $\nu(\text{CC})$ vibration band is observed at 1600 cm^{-1} . Again, the potentiodynamic synthesis results in predominance of the lower energy oxidized structure as opposed to the potentiostatic synthesis. The galvanostatic synthesis produces a mixture of the two components or structures.

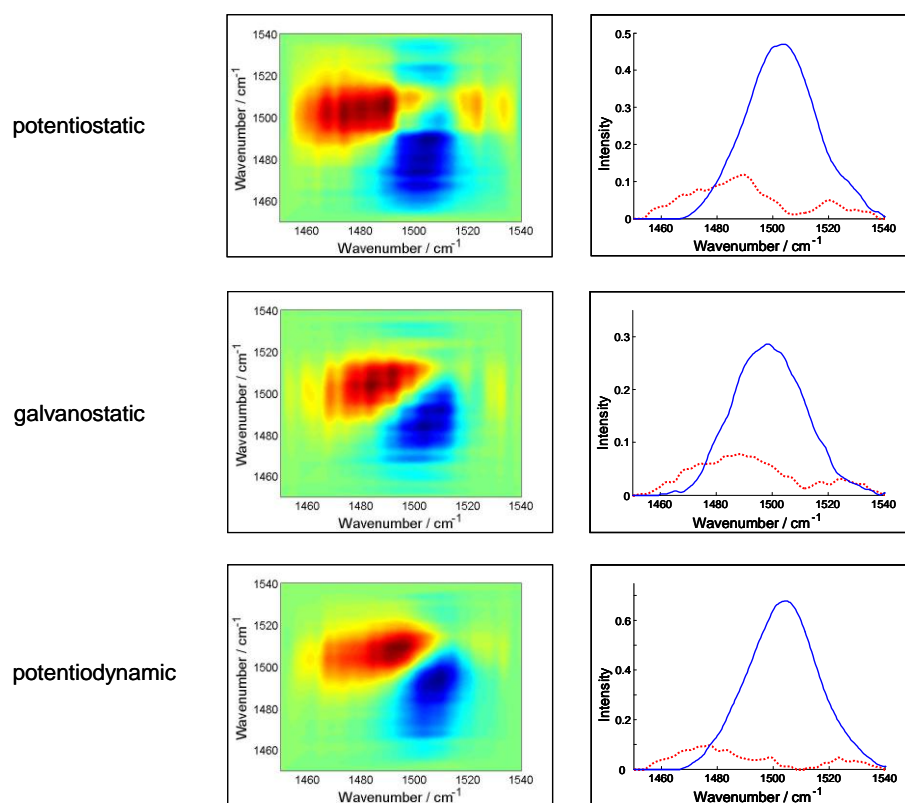


Figure 9. 2D-COS maps and MCR spectral profiles for the $\nu(\text{C}=\text{N})$ stretching and $\delta(\text{NH})$ bending vibrations of electrodeposited PANI

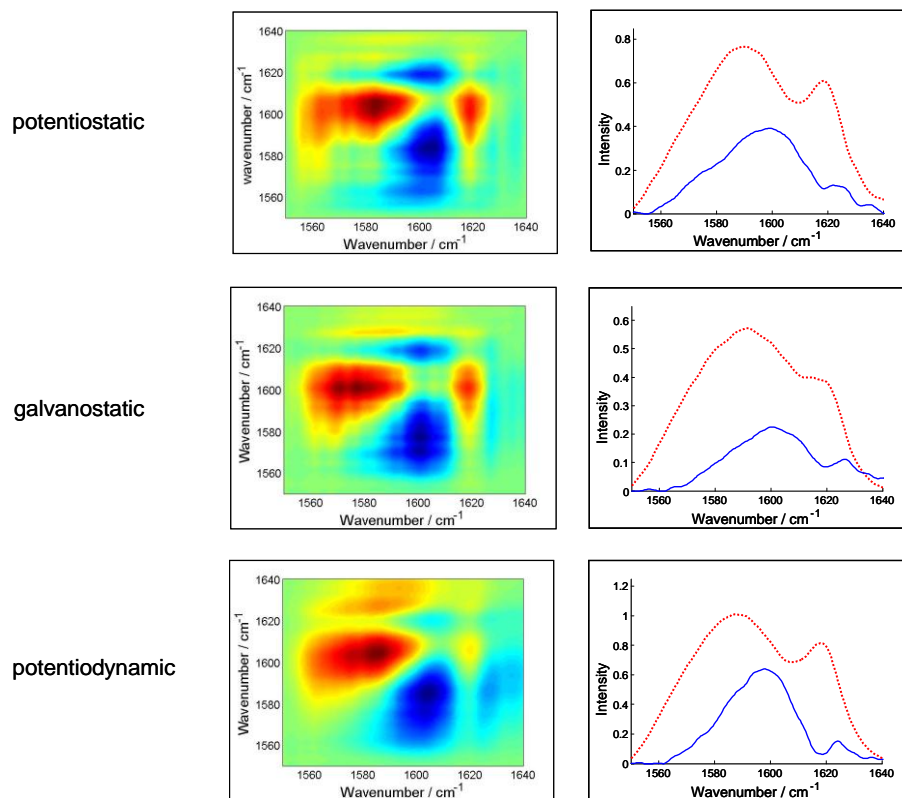


Figure 10. 2D-COS maps and MCR spectral profiles for the $\nu(\text{CC})$ stretching Raman band of electrodeposited PANI

The Raman bands attributed to substituted phenazine structural units have been reported for chemically synthesized PANI at $1630\text{--}1645\text{ cm}^{-1}$ [34]. Our potentiodynamic PANI samples reveal low intensity Raman bands in this range. These bands are not visible in the spectra of potentiostatic samples and same was found using a NMR method for a potentiostatic synthesis of 2-metoxyaniline oligomers [35].

4. CONCLUSIONS

- Electrochemistry indicates the lowest mean conjugation length for the galvanostatic polymer and the thickness dependent properties of electrodeposited polymer films in general.
- The galvanostatic synthesis produces an additional component of the polymer film which is oxidized/reduced at less positive potentials than the mean polymeric material. A complex nature of the polymer films produced under this regime of electrolysis was registered both by cyclic voltammetry and Raman spectroscopy.
- Multivariate analysis of the *in-situ* Raman spectra shows evidently that the electrodeposited PANI films contain mixtures of at least two molecular structures related with a different chemical composition of the polymer chains with their proportions changing in the order:

potentiostatic > galvanostatic > potentiodynamic; *i.e.* in an order of a range of the electrode potential being experienced during the synthesis. The structures in question might be bounded up with the various charged states of emeraldine.

- The 2D-COS method not only confirmed a high complexity of the polaronic band but also showed that the impact of the synthesis conditions on the polaron vibration might have the same origin as for the other analyzed bands. A common explanation for the observed similar patterns for different vibrations might be the chain structure of the polymer affecting different bonds in the chain in a similar way.

References

1. G. Inzelt, *J. Solid State Electrochem.*, 15 (2011) 1711.
2. K. M. Molapo, P. M. Ntangili, R. F. Ajayi, G. Mbambisa, S. M. Mailu, N. Njomo, M. Masikini, P. Baker and E. I. Iwuoha, *Int. J. Electrochem. Sci.*, 7 (2012) 11859.
3. F. Terzi, L. Pasquali and R. Seeber, *Anal. Bioanal. Chem.*, 405 (2013) 1513.
4. M. Baibarac, M. Cochet, M. Łapkowski, L. Mihut, S. Lefrant and I. Baltog, *Synth. Met.*, 96 (1998) 63.
5. Y. Furukawa, F. Ueda, Y. Hyodo, I. Harada, T. Nakaima and T. Kawagoe, *Macromolecules*, 21 (1988) 1297.
6. S. Quillard, K. Berrada, G. Louarn, S. Lefrant, M. Łapkowski and A. Proń, *New J. Chem.*, 19 (1995) 365.
7. M. Zagórska, A. Proń and S. Lefrant, in *Handbook of Organic Conductive Molecules and Polymers*, Vol. 3, H. S. Nalwa (Editor), Wiley (1997) Chichester, p. 183.
8. T. Lindfors, C. Kvarnstrom and A. Ivaska, *J. Electroanal. Chem.*, 518 (2002) 131.
9. L. Dauginet-De Pra and S. Demoustier-Champagne, *Thin Solid Films*, 479 (2005) 321.
10. R. Mazeikiene, V. Tomkute, Z. Kuodis, G. Niaura and A. Malinauskas, *Vib. Spectrosc.*, 44 (2007) 201.
11. M. Grzeszczuk and G. Żabińska-Olszak, *J. Electroanal. Chem.*, 359 (1993) 161.
12. M. Grzeszczuk and P. Poks, *Synth. Met.*, 98 (1998) 25.
13. M. Grzeszczuk and R. Szostak, *Solid State Ionics*, 157 (2003) 257.
14. M. Grzeszczuk and R. Szostak, *J. Electroanal. Chem.*, 571 (2004) 51.
15. D. Fraenkel, *J. Phys. Chem. B*, 116 (2012) 11678.
16. H. R. Keller and D. L. Massart, *Chemom. Intell. Lab. Syst.*, 12 (1992) 209.
17. R. Tauler and A. de Juan, in *Practical Guide to Chemometrics*, P. Gemperline (Editor), CRC Press (2006) Boca Raton, p. 417.
18. I. Noda, *Appl. Spectrosc.*, 47 (1993) 1329.
19. I. Noda and Y. Ozaki, *Two-Dimensional Correlation Spectroscopy - Applications in Vibrational and Optical Spectroscopy*, Wiley (2004) Chichester.
20. M. Shamsipur, B. Hemmateenejad, A. Babaeli and L. Faraj-Sharabiani, *J. Electroanal. Chem.*, 570 (2004) 227.
21. S. J. Hong, Y. M. Jung, S. B. Kim and S. M. Park, *J. Phys. Chem. B*, 109 (2005) 3844.
22. A. P. Bonifas and R. L. McCreery, *Anal. Chem.*, 84 (2012) 2459.
23. Y. O. Kim, Y. M. Jung, S. B. Kim and S. M. Park, *Anal. Chem.*, 76 (2004) 5236.
24. Y. M. Jung, B. Czarnik-Matuszewicz and Y. Ozaki, *J. Phys. Chem. B*, 104 (2000) 7812.
25. R. Szostak, *J. Raman Spectrosc.*, 42 (2011) 1185.
26. M. A. Czarnecki, *Appl. Spectrosc. Rev.*, 46 (2011) 67.
27. G. de T. Andrade, M. J. Aguirre and S. R. Biaggio, *Electrochim. Acta*, 44 (1998) 633.

28. C. Q. Cui, L. H. Ong, T. C. Tan and J. Y. Lee, *J. Electroanal. Chem.*, 346 (1993) 477.
29. K. Kunitatsu, M. G. Samant and H. Seki, *J. Electroanal. Chem.*, 258 (1989) 163.
30. M. I. Boyer, S. Quillard, M. Cochet, G. Louarn and S. Lefrant, *Electrochim. Acta*, 44 (1999) 1981.
31. M. Chmielewski, M. Grzeszczuk, J. Kalenik and A. Kępas-Suwara, *J. Electroanal. Chem.*, 647 (2010) 169.
32. R. Mazeikiene, G. Niaura and A. Malinauskas, *Polym. Degrad. Stab.*, 93 (2008) 1742.
33. E. Dmitrieva and L. Dunsch, *J. Phys. Chem. B*, 115 (2011) 6401.
34. G. Ciric-Marjanovic, M. Trchova and J. Stejskal, *J. Raman Spectrosc.*, 39 (2008) 1375.
35. M. A. del Valle, M. A. Gacitua, E. D. Borrego, P. P. Zamora, F. R. Diaz, M. B. Camarada, M. P. Antilen and J. P. Soto, *Int. J. Electrochem. Sci.*, 7 (2012) 2552.